
Imaging diffuse liver disease

Rishi Philip Mathew, MBBS, DMRD, EDiR; and Sudhakar K Venkatesh, MD, FRCR

Many pathophysiological processes can lead to diffuse parenchymal liver diseases and the end-result of all chronic liver diseases (CLD) is healing by fibrosis and regeneration.¹ Hepatic fibrosis, left untreated, progresses to cirrhosis and its associated complications, a major cause of death worldwide. For an effective cure, hepatic fibrosis should be diagnosed early and monitored during treatment. Liver biopsy is the gold standard but limited due to its invasiveness, sampling error, and intra- and interobserver variability. Non-invasive tests are preferred in the management of CLD.^{2,3,4} Several serum tests for liver function and markers of liver fibrosis are available and have moderate sensitivity and specificity; however, they are confounded by a wide range of extrahepatic diseases.⁵ Imaging plays an important role in evaluation of CLD and its complications.

Conventional ultrasound (US), computed tomography (CT) and magnetic

resonance imaging (MRI) are routinely used to evaluate CLD. These methods assess morphological changes in the liver that are typically seen in the advanced stages (cirrhosis) and are not sensitive for detection of early hepatic fibrosis. However, US, CT, and MRI are excellent methods for evaluating complications, including portal hypertension, ascites and hepatocellular carcinoma. For early detection, quantitative techniques are most useful. MRI is the most promising technique for quantification of hepatic steatosis, iron overload, and hepatic fibrosis.^{6,7}

Non-alcoholic fatty liver disease (NAFLD) is now the most common cause of CLD and the leading cause of liver transplantation. NAFLD is a major health burden worldwide, with great implications for medical resources, and is the most common CLD encountered by radiologists.^{8,9} In this review, we will briefly review the quantitative assessment of hepatic steatosis and iron overload and focus on current and emerging techniques for evaluation of liver fibrosis.

Hepatic steatosis

In the normal liver 5% or fewer hepatocytes have fatty change. Hepatic steatosis or fatty liver results from excessive accumulation of triglycerides

within hepatocytes, and a condition that affects nearly 25-35% of the US population.¹⁰ Hepatic steatosis can result from many causes including alcohol, drugs, storage disorders, infection and pregnancy. The most common cause of hepatic steatosis is NAFLD, which is associated with obesity and metabolic syndrome.¹⁰ NAFLD is a spectrum of disease, with 70-80% of patients having the benign, non-progressive non-alcoholic fatty liver (NAFL). About 20-30% of have progressive non-alcoholic steatohepatitis (NASH), characterized by inflammation and ballooning of hepatocytes, and about 5% of NASH patients progress to cirrhosis.^{11,12} NAFLD patients are also susceptible to liver failure, as well as cardiovascular and renal comorbidities.¹³ As hepatic steatosis is a biomarker of NAFLD, detection and quantification of fat is important.

Ultrasound is useful for detecting fatty change in the liver; however, the increased echogenicity of the liver parenchyma is nonspecific. In addition, the quantification of fatty changes with grayscale ultrasound is inaccurate. A new technique, controlled attenuation parameter (CAP), is now available with elastography to quantify the liver fat. CAP can easily detect steatosis >10%.¹⁴

Dr. Mathew is a Clinical Fellow in Body Imaging, in the Department of Radiology & Diagnostic Imaging, at the University of Alberta Hospital, Edmonton, Alberta, Canada; and Dr. Venkatesh is a Professor of Radiology at the Mayo Clinic College of Medicine, Rochester, MN. The authors have no conflicts of interest to disclose.

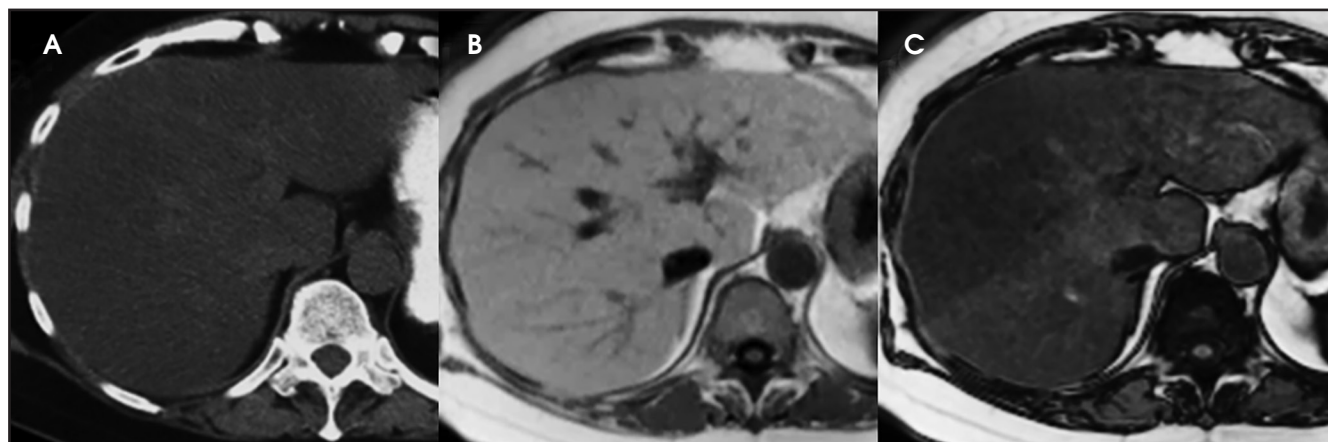


FIGURE 1. Unenhanced CT (A), axial In-phase (B) and opp-phase (C) images at the same level in a patient with hepatic steatosis. Hepatic steatosis causes diffuse hypo-attenuation of the liver and vessels appear denser and on MRI there is loss of signal in opp-phase. Note the heterogeneity of steatosis.

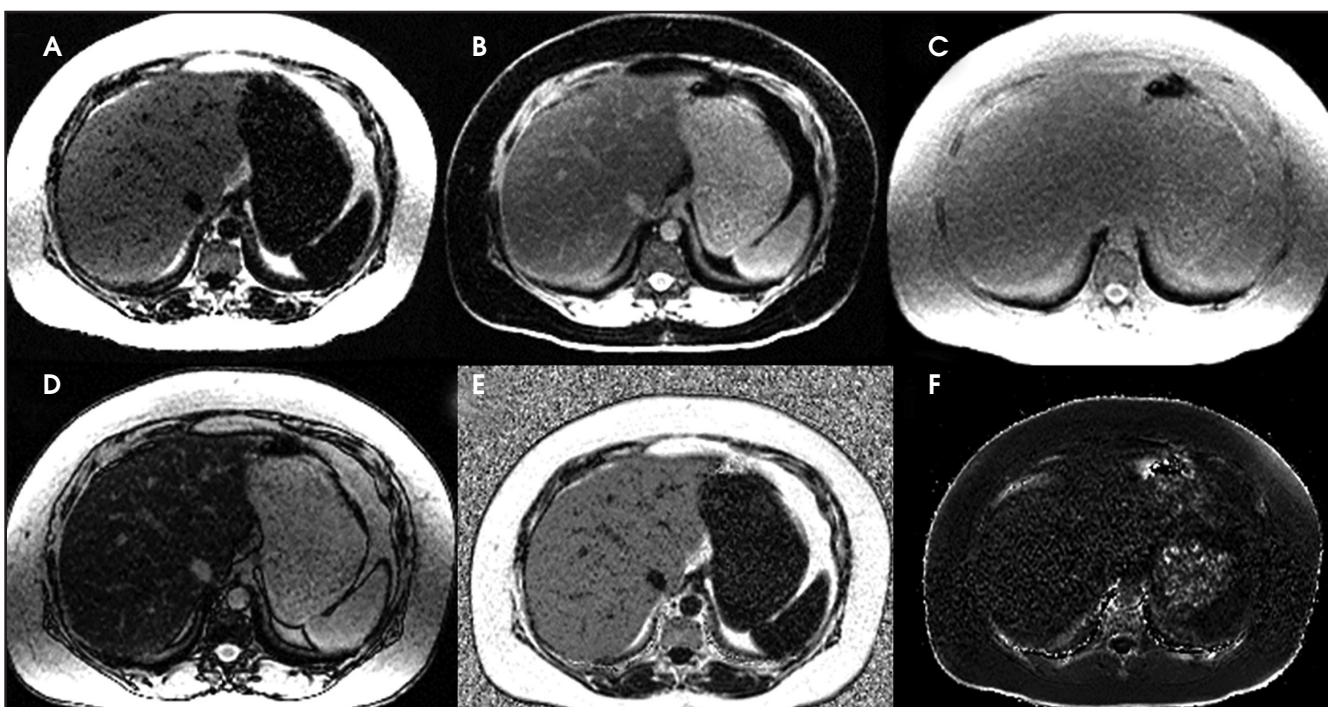


FIGURE 2. Chemical shift encoded multi-echo sequence produces multiple images, including (A) fat, (B) water, (C) In-phase, (D) opp-phase, (E) fat fraction map, and (F) R2* map.

The utility of CAP for hepatic steatosis is still being evaluated.

The attenuation of a normal healthy liver on non-contrast enhanced CT ranges from 50-65 Hounsfield Units (HU) and is denser than the spleen parenchyma and the hepatic vasculature.^{15,16} Non-contrast CT is more accurate in qualitatively diagnosing moderate to severe hepatic steatosis than it is in mild to moderate steatosis. Hepatic steatosis can

be diagnosed when liver attenuation < spleen attenuation or when liver attenuation < 48 HU.¹⁵ Increased density of the liver vessels compared to the liver parenchyma (Figure 1) is associated with 30% steatosis. Moderate-to-severe hepatic steatosis can be diagnosed with 100% specificity when liver attenuation is <40-42 HU, hepatic-spleen attenuation ratio is < 0.8, or a hepatic-spleen attenuation difference is \leq -10 HU with 73-82% sen-

sitivity for moderate-to-severe hepatic steatosis.^{17,18} Due to the risks associated with ionizing radiation exposure, CT is not recommended for evaluating hepatic steatosis.

MRI is the most useful technique for evaluating hepatic steatosis. The various techniques for detecting and quantifying hepatic steatosis include fat suppression, chemical shift imaging (CSI), frequency selective imaging, and

Table 1. MRI techniques for fat quantification.

Method	Advantages	Disadvantages
In-phase and opposed-phase imaging	<ul style="list-style-type: none"> • Simple technique • Whole liver 	<ul style="list-style-type: none"> • Fat quantification may be unreliable when IP is acquired before OP • Confounding factors: Iron
Frequency selective imaging (fat suppression technique)	<ul style="list-style-type: none"> • Simple technique • Easily combined with other sequences 	<ul style="list-style-type: none"> • Requires a homogeneous magnetic field for uniform suppression • Requires distinct separation of fat and water spectral peaks
Magnetic resonance spectroscopy (MRS)	<ul style="list-style-type: none"> • Minute fat as low as 0.5% detectable • High accuracy over a wide range of hepatic steatosis 	<ul style="list-style-type: none"> • Quality dependent on magnetic field uniformity • Sampling error • Susceptibility artifacts • Need for technical expertise • Additional processing time
Chemical shift encoded PDFF estimation	<ul style="list-style-type: none"> • Wide range of hepatic steatosis assessed (0-100%) • Automated generation of R2*, water, fat, IP, OP images • High accuracy, similar to MRS 	<ul style="list-style-type: none"> • Presence of confounders, especially moderate to severe iron, may affect quantification • Not available in all MRI scanners

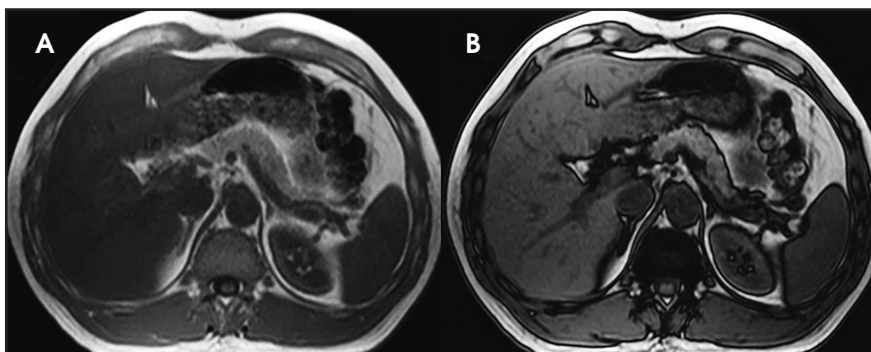


FIGURE 3. Axial In- (A) and opposed- phase (B) images in a patient with iron overload due to hemochromatosis. Note the loss of signal of liver parenchyma in the in-phase.

MR spectroscopy (MRS). Qualitative in-phase and opposed-phase imaging (IP/OP) is widely available and can easily detect fat in the liver (Figure 1). However, the range of hepatic steatosis that can be quantified is only 0-50% and the sequence is easily affected by the presence of iron and other paramagnetic substances. MRS is the most accurate imaging technique capable of detection of small quantities of liver fat and for followup.^{18,19} However, MRS analysis is limited to a single anatomical location, requires technical expertise and additional post-processing time. Hence, MRS remains a major research tool widely used in clinical trials and not in routine clinical practice.

The accuracy of proton density fat fraction (PDFF) measurement using chemical shift encoded methods is similar to that of MRS and is easily implemented in MRI scanners. These are typically performed with single-breath-hold sequences that allow coverage of the entire liver. Unlike the previously mentioned MRI techniques, PDFF pulse sequences have been optimized such that they are minimally affected by magnetic field inhomogeneity and T2* effects. A recent study conducted by Serai et al²⁰ showed that PDFF estimation using multipoint Dixon techniques was highly reproducible across readers, magnetic field strengths and across vendor imaging platforms. The advantage

of these multi-echo-based sequences is that, in addition to PDFF, they also generate R2* (or T2*) maps, IP and OP images, and water and fat images (Figure 2). The ease of quantification by drawing regions of interest (ROI) over liver parenchyma makes it practical for clinical use. The advantages and disadvantages of various MRI techniques for the quantification of fat is summarized in Table 1.^{21,22}

Hepatic iron overload

Liver iron overload results from abnormal accumulation of iron in the hepatocytes, Kupffer cells, or both.²³ The condition is associated mostly with hereditary hemochromatosis, transfusion-related iron overload, and chronic liver pathologies.²⁴ Ultrasound is not a suitable modality for evaluating liver iron overload, as it cannot detect iron deposits. On non-contrast CT, iron overload results in increased liver density (\geq HU); however, co-existent hepatic steatosis, which commonly presents as reduced attenuation on CT, can reduce detection sensitivity. Similarly, other pathologies that can increase the liver density on CT, such as Wilson disease, colloidal gold treatment and amiodarone administra-

Table 2. Summary of ultrasound elastography techniques

Technique	Advantages	Limitations
Vibration controlled transient elastography (TE)	<ul style="list-style-type: none"> • Rapid (< 5 mins) • Portable and point of care • Results are immediately available • Reliable in the assessment of advanced liver fibrosis 	<ul style="list-style-type: none"> • Multiple successful measurements must be obtained within a defined interquartile range to obtain a valid result • No real-time imaging guidance; hence, no anatomical information • Obesity • Ascites • Confounding factors including fatty change, inflammation, and cholestasis
Static or quasistatic strain imaging/compression elastography	<ul style="list-style-type: none"> • Mainly used for breast and thyroid imaging 	<ul style="list-style-type: none"> • Variable compression • Limited role in liver imaging, as intercostal space and subcutaneous fat thickness hinder compression
Point shear wave elastography (pSWE)	<ul style="list-style-type: none"> • Allows ROI selection • Follow up at same spot possible • More robust shear wave production than VCTE • Diagnostic performance similar to VCTE 	<ul style="list-style-type: none"> • Requires more expertise than one-dimensional transient elastography • Needs more validation • Tissue energy absorption is greater than one-dimensional transient elastography; concerns for tissue heating
Shear wave elastography (SWE)	<ul style="list-style-type: none"> • Larger ROI • Shear waves measured using real time imaging • Produces a 2D map when the passing shear wave is measured • Real-time color map of tissue viscoelastic properties under evaluation • Less impact from obesity and ascites 	<ul style="list-style-type: none"> • Requires more expertise of sonographers • Less validated when compared to TE • Not currently used for diagnostic purposes in clinical practice

tion, can decrease the specificity of CT. Consequently, CT is not considered a reliable modality for the diagnosis and quantification of liver iron overload.

MRI is a well-established modality for assessing liver iron concentration (LIC) and is a good alternative to biopsy. IP/OP images, which are part of standard liver MRI protocols, can also detect iron. A signal drop is noted on IP images in the case of iron (Figure 3), while fat causes a signal drop on OP images. Iron causes shortening of T1, T2, and T2*, and this shortening is more pronounced with T2* images. Therefore, T2*-weighted images have higher sensitivity and are more routinely used for detecting iron.^{25,26} The two major methods used in quantifying liver iron overload are signal intensity ratio (SIR) and relaxometry. SIR method calculates the signal intensity (SI) of the liver and another tissue

with no iron accumulation (eg, muscle) and determines the ratio to quantify the LIC.^{27,28} Limitations of SIR include its inability to quantify LIC >350 μmol Fe/g and tendency to overestimate LIC. Relaxometry methods, on the other hand, calculate the SI of the liver across several echo times and measure the T2 or T2* values depending on the obtained sequence. T2 or T2* values are inversely related to iron concentration. But, R2 or R2* values (1000/T2 or T2*) are directly related to the iron concentration and increase linearly with LIC determined by liver biopsy. R2* and T2* calculation plays a crucial role in identifying the extent of LIC for treatment with iron-chelating agents. The major advantage of relaxometry is its ability to also calculate myocardial iron overload, while its limitations include the requirement of specialized software which is not

readily available.²⁹ A T2* value <18ms is considered to be liver iron overload.³⁰ A recent study conducted by Galimberti et al³¹ showed that an R2* cut-off value of 147.1 Hz (T2* value of 6.8ms) discriminates moderate and severe hepatic iron overload from absent and mild hepatic iron overload. MR field strength is an important factor in measuring LIC. Although high field strengths have an advantage in identifying tissues with low iron content, the susceptibility to artifacts reduces the sensitivity for detection and quantification of severe iron overload.^{32,33} Chemical shift-encoded sequences that automatically generate PDFF and R2* maps for fat and iron quantification, respectively, are useful for clinical practice without the need for additional post-processing. Liver iron quantification with MRI should be tailored to the clinical need and benchmarked against the institutional

Table 3. Confounders of ultrasound elastography**Technical confounders**

1. *Left lobe vs. right lobe measurements*
Left lobe measurements are associated with a higher liver stiffness measurement due to liver compression by the transducer, heart, or stomach.
2. *Depth of measurement*
Measurements of high stiffness were noted closer to the liver surface compared to deeper measurements. Stiffness measurements ≥ 1 cm below liver surface are recommended.
3. *Wave frequencies*
The liver shows a dispersive (ie, frequency-dependent) behavior. Therefore, the choice of excitation frequency is vital in liver elastography to obtain the frequency- dependent viscoelastic properties.
4. *Device dependencies and standardization*
Shear-wave speed measurement is not yet standardized across modalities, scanners, and transducers.

Biological confounders

1. *Hepatic steatosis*
The effect of steatosis on liver stiffness remains controversial.
2. *Inflammation*
Inflammation, particularly acute inflammation, can lead to increase in elasticity and viscosity.
3. *Cholestasis*
Liver stiffness can also be increased by extrahepatic cholestasis.
4. *Breathing*
Deep inspiration can lead to erroneous liver stiffness measurements; hence, breath hold at end expiration is preferred to prevent overestimating liver stiffness.
5. *Right heart failure*
Right heart failure is associated with increased liver stiffness.
6. *Hepatic venous congestion*
Hepatic venous congestion can also increase liver stiffness.
7. *Fasting vs. postprandial state*
In patients with chronic liver disease, postprandial state can increase liver stiffness; hence, liver stiffness should be measured preferably in the fasting state.

laboratory values of serum and blood iron levels, as the test results are variable with different laboratory equipment.

Hepatic fibrosis and cirrhosis

CLDs are characterized by ongoing inflammation and fibrosis. Chronic inflammation leads to potentially reversible early hepatic fibrosis and when untreated progresses to cirrhosis with the cross-linking of collagen fibres and the formation of regenerative nodules.³⁴ Regression of hepatic fibrosis can occur, with significant reduction in fibrosis burden, especially when treatment is started early. Hepatitis C can be cured with new antiviral drugs and lifestyle changes can significantly reduce hepatic steatosis. Non-invasive detection and staging of hepatic fibrosis is important in the management of chronic liver diseases.

Ultrasound (US)

Liver fibrosis causes coarse echogenicity of liver parenchyma on US, a nonspecific feature that can be seen with fatty change and inflammation. Although grayscale US can identify a cirrhotic liver in CLD, it is unreliable for identifying mild changes,^{35,36} and is often unable to differentiate between mild and severe fibrosis.³⁷ US however can detect morphological changes in advanced fibrosis with moderate accuracy.³⁸

Ultrasound-based elastography

Ultrasound-based Elastography methods include vibration controlled transient elastography (VCTE), point shear wave elastography (pSWE) and shear wave elastography (SWE). These are simple to use and can detect liver cirrhosis with high accuracy. The

advantages and limitations of VCTE, pSWE and SWE have been summarized in Table 2.³⁹ Although US elastography is an inexpensive and accurate technique for diagnosing liver cirrhosis, it has significant limitations and confounders (Tables 2,3). The methods are operator-dependent and in general have reduced sensitivity and specificity in detecting early fibrosis.^{40,41}

Computed tomography (CT)

Diagnosing fibrosis/cirrhosis on CT relies on morphological changes, such as irregular or nodular liver surface, blunt edges, heterogeneous texture, widened fissures, segmental atrophy and hypertrophy and features of portal hypertension.⁴² CT is useful for evaluating complications such as esophageal varices, hepatocellular carcinoma, and ascites. Nevertheless, CT is not the preferred

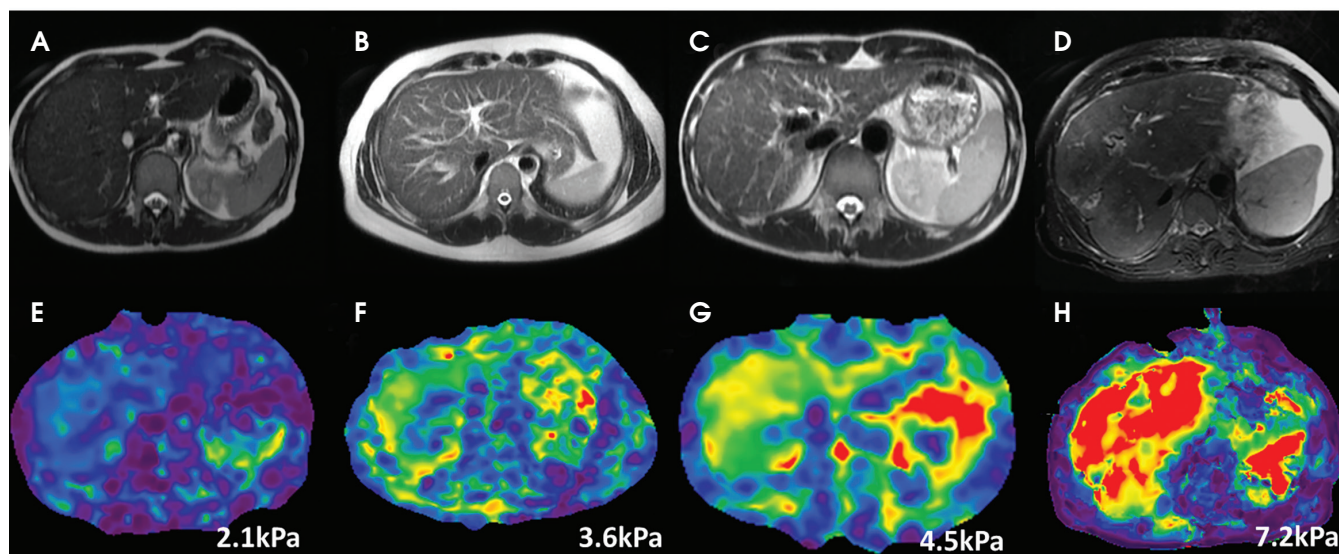


FIGURE 4. Axial T2-weighted MRI images of normal healthy volunteer (A), stage 2 fibrosis (B), stage 3 fibrosis (C), and stage 4 fibrosis (D). Corresponding MRE stiffness maps (E-H). Numbers in right lower corners are mean stiffness of liver parenchyma.

Table 4. Clinically useful liver stiffness measurement cut-offs with MRE

MRE Stiffness (kPa)	Fibrosis Stage
< 2.5	Normal
2.5- 2.9	Normal or inflammation
2.9-3.5	Stage 1-2
3.5-4.0	Stage 2-3
4.0-5.0	Stage 3-4
> 5.0	Stage 4

modality for primary diagnosis of liver fibrosis because of the risk of radiation and its lower sensitivity for early hepatic fibrosis. Clinically occult liver fibrosis is often underdiagnosed in routine abdominal CT, and its sensitivity (77.1%–84.3%) and specificity (52.9%–67.6%) for liver cirrhosis is mediocre.⁴³

Magnetic resonance imaging (MRI)

Conventional MRI probably has slightly better accuracy than CT as parenchymal heterogeneity due to underlying fibrosis can be better appreciated on MRI sequences which helps to detect earlier stages of fibrosis. However, conventional MRI is still limited in the detection of early hepatic fibrosis and hence, not reliable for disease staging. Newer MR imaging techniques such as diffusion-weighted imaging (DWI), perfusion imaging, texture analysis,

hepatocellular function imaging, t1- ρ imaging, susceptibility weighted imaging (SWI) and MR elastography are now being explored for application in hepatic fibrosis.^{44,45}

Diffusion weighted imaging is useful for identifying advanced fibrosis and cirrhosis, but the technique lacks standardization across platforms and has low accuracy, as apparent diffusion coefficient (ADC) values overlap between normal liver and fibrotic/cirrhotic liver.⁴⁶ Extrapolating the DWI technique, utilizing several b-values an intravoxel incoherent motion (IVIM) analysis is performed, especially with low b-values (<200 s/mm²). Several studies have evaluated the relationship between ADC and fibrosis stage, with conflicting results.⁴⁶ While some studies have noted a reduction in ADC values with increasing fibrosis stage, a study⁴⁶ observed this pattern only in

live, not dead, rats, suggesting that perfusion rather than diffusion is affected by fibrosis stage. DWI and IVIM techniques are limited by lack of standardization and have confounding factors of fat and iron deposition in the liver.⁴⁷

MR elastography (MRE)

MRE of the liver was introduced into clinical practice in 2007. MRE is currently the most accurate non-invasive MRI technique for detecting and staging of liver fibrosis.^{29,38,48} MRE can reliably differentiate NAFLD from NASH prior to patients developing liver fibrosis.⁴⁹ Similar to ultrasound based shear wave elastography, MRE utilizes propagating shear waves produced by a vibrating passive driver placed over the liver and imaged with a special phase encoded MRI sequence. The wave information is automatically processed with software and produces maps for liver stiffness measurement.⁵⁰ Liver stiffness increases in higher stages of fibrosis and is easily distinguishable from normal liver stiffness (<2.5kPa) (Figure 4). Liver stiffness measurement with MRE has proven to have a higher sensitivity and specificity for each stage of fibrosis when compared to DWI.⁵¹ MRE has 98% sensitivity and 99% specificity detection of hepatic fibrosis and is considered an alternative gold standard to

liver biopsy. MRE can be easily added to standard liver MRI protocols, allows a large sample of liver to be assessed, is not influenced by ascites, obesity or hepatic steatosis, is unaffected by intravenous contrast administration, and has high intra- and interobserver agreement for measurement of stiffness. However, MRE has a few limitations and these include potential failure in patients with moderate-to-severe iron accumulation due to low signal of the liver parenchyma, additional time required for positioning the driver, and lack of availability at all centres. Clinically useful LSM cut-offs are provided in Table 4.

MRI techniques estimating fractional extracellular space estimation⁵² and magnetic transfer ratio (MTR) have been less successful in differentiating normal from cirrhotic liver.⁵³ MR perfusion requires the use of intravenous contrast and early studies have reported encouraging results⁵⁴ but has technical limitations, requires patient co-operation for several breath holds and is susceptible to motion artifacts. Perfusion imaging is also not widely available.

T1 ρ imaging is another MRI technique which uses the spin-lattice relaxation time for evaluation of hepatic fibrosis. It has been shown useful for hepatic fibrosis staging, as demonstrated by a preclinical study conducted on rat livers.⁵⁵ Preliminary T1 ρ MRI studies have shown that, compared to normal liver, fibrotic liver exhibits higher T1 ρ values and has high diagnostic accuracy to differentiate normal from cirrhotic livers.^{56,57} However, this technique is influenced by magnetic field inhomogeneity and breath-hold artifacts. Further evaluation with more subjects is required to establish its role in assessing liver fibrosis.

Texture analysis is an emerging method for evaluation of hepatic fibrosis and can be performed with any technique. Currently there is no standardized approach and several different software methods exist. Diagnostic performance of texture analysis is variable.^{58,59}

Hepatocellular function imaging can be performed easily on any clinical

MRI scanner; however, this requires hepatobiliary contrast medium—gadoxetate sodium—that is invasive and adds scan time. Relative enhancement parameters are derived from hepatobiliary phase and non-contrast-enhanced T1-weighted images. The enhancement is reduced in hepatic fibrosis and cirrhosis. Early studies have been encouraging and shown high accuracy of 0.93 for diagnosis of advanced fibrosis. This technique needs further evaluation.

Conclusion

Recent advances in diagnostic imaging have led to an early and improved detection of diffuse liver diseases. MRI is the main modality for imaging diffuse liver diseases and provides accurate quantification of liver fat, iron, and fibrosis.

REFERENCES

1. Boll DT, Merkle EM. Diffuse liver disease: strategies for hepatic CT and MR imaging. *Radiographics*. 2009;29(6):1591-1614.
2. Van Beers BE, Daire JL, Garteiser P. New imaging techniques for liver diseases. *J Hepatol*. 2015(3);62:690-700.
3. Ba-Ssalamah A, Bastati N, Wibmer A, et al. Hepatic gadoxetic acid uptake as a measure of diffuse liver disease: Where are we? *J Magn Reson Imaging*. 2017;45(3):646-659.
4. Ratziu V, Charlotte F, Heurtier A, et al. Sampling variability of liver biopsy in nonalcoholic fatty liver disease. *Gastroenterology*. 2005;128(7):1898-1906.
5. Rosenberg WM, Voelker M, Thiel R, et al. Serum markers detect the presence of liver fibrosis: a cohort study. *Gastroenterology*. 2004;127(6):1704-1713.
6. Bashir MR, Zhong X, Nickel MD, et al. Quantification of hepatic steatosis with a multistep adaptive fitting MRI approach: prospective validation against MR spectroscopy. *AJR Am J Roentgenol*. 2015;204(2):297-306.
7. Ma X, Holalkere NS, Kambadakone A, et al. Imaging based quantification of hepatic fat: methods and clinical applications. *RadioGraphics*. 2009;29(5):1253-1280.
8. Lall CG, Aisen AM, Bansal N, et al. Nonalcoholic fatty liver disease. *AJR Am J Roentgenol*. 2008;190(4):993e1002.
9. Nobili V, Alisi A, Newton KP, et al. Comparison of the phenotype and approach to pediatric vs adult patients with non-alcoholic fatty liver disease. *Gastroenterology*. 2016;150(8):1798-1810.
10. Hassan K, Bhalla V, El Regal ME, et al. Non-alcoholic fatty liver disease: a comprehensive review of a growing epidemic. *World J Gastroenterol*. 2014;20(34):12082-12101.
11. Petaja EM, Yki-Jarvinen H. Definitions of normal liver fat and the association of insulin sensitivity with acquired and genetic NAFLD-A systematic review. *Int J Mol Sci*. 2016;17(5): pii: E633.
12. Oda K, Uto H, Mawatari S, et al. Clinical features of hepatocellular carcinoma associated with nonalcoholic fatty liver disease: a review of human studies. *Clin J Gastroenterol*. 2015;8(1):1-9.
13. Fotbolcu H, Zorlu E. Nonalcoholic fatty liver disease as a multisystemic disease. *World J Gastroenterol*. 2016;22(16):4079-4090.
14. Sasso M, Beaugrand M, de Ledinghen V, et al. Controlled attenuation parameter (CAP): a novel VCTE™ guided ultrasonic attenuation measurement for the evaluation of hepatic steatosis: preliminary study and validation in a cohort of patients with chronic liver disease from various causes. *Ultrasound Med Biol*. 2010;38(11):1825-1835.
15. Valls C, Iannaccone R, Alba E, et al. Fat in the liver: diagnosis and characterization. *Eur Radiol*. 2006;16(10):2292e308.
16. Schwenzer NF, Springer F, Schraml C, et al. Non-invasive assessment and quantification of liver steatosis by ultrasound, computed tomography and magnetic resonance. *J Hepatol*. 2009;51(3):433e45.
17. Kani KK, Moshiri M, Cuevas C, et al. Imaging patterns of hepatic steatosis on multidetector CT: pearls and pitfalls. *Clin Radiol*. 2012;67(4):366-371.
18. Mehta SR, Thomas EL, Bell JD, et al. Non-invasive means of measuring hepatic fat content. *World J Gastroenterol*. 2008;14(22):3476-3483.
19. Schwenzer NF, Springer F, Schraml C, et al. Non-invasive assessment and quantification of liver steatosis by ultrasound, computed tomography and magnetic resonance. *J Hepatol*. 2009;51(3):433-445.
20. Serai SD, Dillman JR, Trout AT. Proton density fat fraction measurements at 1.5- and 3-T hepatic MR imaging: same-day agreement among readers and across two imager manufacturers. *Radiology*. 2017;284(1):244-254.
21. Cassidy FH, Yokoo T, Aganovic L, et al. Fatty liver disease: MR imaging techniques for the detection and quantification of liver steatosis. *Radiographics*. 2009;29(1):231-260.
22. Gangadhar K, Kedar N. Chintapalli, et al. MRI evaluation of fatty liver in day to day practice: Quantitative and qualitative methods. *Egypt J Radiol Nucl Med*. 2014;45(3):619-626.
23. Brittenham GM, Cohen AR, McLaren CE, et al. Hepatic iron stores and plasma ferritin concentration in patients with sickle cell anemia and thalassemia major. *Am J Hematol*. 1993; 42(1):81-85.
24. Adams P, Brissot P, Powell LW. EASL International Consensus Conference on Haemochromatosis. *J Hepatol*. 2000; 33(3):485-504.
25. Hernando D, Levin YS, Sirlin CB, et al. Quantification of liver iron with MRI: state of the art and remaining challenges. *J Magn Reson Imaging*. 2014;40(5):1003-1021.
26. Sirlin CB, Reeder SB. Magnetic resonance imaging quantification of liver iron. *Magn Reson Imaging Clin N Am*. 2010;18(3):359-381, ix.
27. Gandon Y, Olivieri D, Guyader D, et al. Non-invasive assessment of hepatic iron stores by MRI. *Lancet*. 2004;363(9406):357-362.
28. Paisant A, Boulic A, Bardou-Jacquet E, et al. Assessment of liver iron overload by 3 T MRI. *Abdom Radiol (NY)*. 2017;42(6):1713-1720.
29. Tan CH, Venkatesh SK. Magnetic resonance elastography and other magnetic resonance imaging techniques in chronic liver disease: Current status and future directions. *Gut Liver*. 2016;10(5):672-686.

30. İdilman İS, Akata D, Özmen MN, et al. Different forms of iron accumulation in the liver on MRI. *Diagn Interv Radiol*. 2016;22(1):22-28.
31. Galimberti S, Trombini P, Bernasconi DP, et al. Simultaneous liver iron and fat measures by magnetic resonance imaging in patients with hyperferritinemia. *Scand J Gastroenterol*. 2015; 50(4):421-438.
32. Meloni A, Positano V, Keilberg P. Feasibility, reproducibility, and reliability for the T2* iron evaluation at 3T in comparison with 1.5T. *Magn. Reson. Med*. 2012;68(2): 543-551.
33. Taouli B, Ehman RL, Reeder SB. Advanced MRI methods for assessment of chronic liver disease. *AJR Am J Roentgenol*. 2009;193(1):14-27.
34. Hung CH, Lu SN, Wang JH, Lee CM, Chen TM, Tung HD, Chen CH, Huang WS, Changchien CS. Correlation between ultrasonographic and pathologic diagnoses of hepatitis B and C virus-related cirrhosis. *J Gastroenterol*. 2003;38(2):153-7.
35. Nicolau C, Bianchi L, Vilana R. Gray-scale ultrasound in hepatic cirrhosis and chronic hepatitis: diagnosis, screening, and intervention. *Semin Ultrasound CT MR*. 2002;23(1):3-18.
36. Zheng RQ, Wang QH, Lu MD, et al. Liver fibrosis in chronic viral hepatitis: an ultrasonographic study. *World J Gastroenterol*. 2003;9(11): 2484-2489.
37. Choong CC, Venkatesh SK, Siew EP. Accuracy of routine clinical ultrasound for staging of liver fibrosis. *J Clin Imaging Sci*. 2012;2:58. doi: 10.4103/2156-7514.101000. Epub 2012.
38. Tang A, Cloutier G, Szeverenyi NM, et al. CB. Ultrasound elastography and MR elastography for assessing liver fibrosis: Part 1, principles and techniques. *AJR Am J Roentgenol*. 2015;205(1): 22-32.
39. Srinivasa Babu A, Wells ML, Teytelboym OM, et al. Elastography in chronic liver disease: modalities, techniques, limitations, and future directions. *Radio-graphics*. 2016;36(7):1987-2006.
40. Huber A, Ebner L, Heverhagen JT, et al. State-of-the-art imaging of liver fibrosis and cirrhosis: A comprehensive review of current applications and future perspectives. *EJR Open*. 2015;2:90-100.
41. Kreuer S, Elgethun M, Tommack M. Imaging findings of cirrhosis. *J AM Osteopath Coll Radiol*. 2016;5(2):5-13.
42. Huber A, Ebner L, Montani M, et al. Computed tomography findings in liver fibrosis and cirrhosis. *Swiss Med Wkly*. 2014; 19;144:w13923.
43. Kudo M, Zheng RQ, Kim SR, et al. Diagnostic accuracy of imaging for liver cirrhosis compared to histologically proven liver cirrhosis. *Intervirolgy*. 2008;51(Suppl. 1):17-26.
44. Yeom SK, Lee CH, Cha SH, et al. Prediction of liver cirrhosis, using diagnostic imaging tools. *World J Hepatol*. 2015;7(17):2069-2079.
45. Sandrasegaran K. Functional MR imaging of the abdomen. *Radiol Clin North Am*. 2014;52(4): 883-903.
46. Annet L, Peeters F, Abarca-Quinones J, et al. Assessment of diffusion weighted MR imaging in liver fibrosis. *J Magn Reson Imaging*. 2007;25(1):122-128.
47. Bulow R, Mensel B, Meffert P, et al. Diffusion weighted magnetic resonance imaging for staging liver fibrosis is less reliable in the presence of fat and iron. *Eur Radiol*. 2013;23(5):1281-1287.
48. Wang QB, Zhu H, Liu HL, et al. Performance of magnetic resonance elastography and diffusion-weighted imaging for the staging of hepatic fibrosis: a meta-analysis. *Hepatology*. 2012;56(1):239-247.
49. Chen J, Talwalkar JA, Yin M, et al. Early detection of nonalcoholic steatohepatitis in patients with nonalcoholic fatty liver disease by using MR elastography. *Radiology*. 2011;259(3):749-756.
50. Venkatesh SK, Yin M, Ehman RL. Magnetic resonance elastography of liver: Technique, analysis and clinical applications. *J Magn Reson Imaging*. 2013;37(3):544-555.
51. Wang Y, Ganger DR, Levitsky J, et al. Assessment of chronic hepatitis and fibrosis: comparison of MR elastography and diffusion-weighted imaging. *Am J Roentgenol*. 2011;196(3):553-561.
52. Varenika V, Fu Y, Maher JJ, et al. Hepatic fibrosis: evaluation with semiquantitative contrast-enhanced CT. *Radiology*. 2013;266(1):151-158.
53. Rosenkrantz AB, Storey P, Gilet AG, et al. Magnetization transfer contrast-prepared MR imaging of the liver: inability to distinguish healthy from cirrhotic liver. *Radiology*. 2012;262(1):136-143.
54. Ou HY, Bonekamp S, Bonekamp D, et al. MRI arterial enhancement fraction in hepatic fibrosis and cirrhosis. *Am J Roentgenol*. 2013; 201(4):596-602.
55. Wang YX, Yuan J, Chu ES, et al. T1rho MR imaging is sensitive to evaluate liver fibrosis: an experimental study in a rat biliary duct ligation model. *Radiology*. 2011;259(3):712-719.
56. Singh A, Reddy D, Haris M, et al. T1ρ MRI of healthy and fibrotic human livers at 1.5 T. *J Transl Med*. 2015;13:292.
57. Rauscher I, Eiber M, Ganter C, et al. Evaluation of T1ρ as a potential MR biomarker for liver cirrhosis: comparison of healthy control subjects and patients with liver cirrhosis. *Eur J Radiol*. 2014;83(6):900-904.
58. Yokoo T, Wolfson T, Iwaisako K, et al. Evaluation of liver fibrosis using texture analysis on combined contrast enhanced magnetic resonance images at 3.0T. *Biomed Res Int*. 2015; 387653.
59. Kato H, Kanematsu M, Zhang X, et al. Computer-aided diagnosis of hepatic fibrosis; Preliminary evaluation of MRI texture analysis using the finite difference method and an artificial neural network. *Am J Roentgenol*. 2007; 189(1):117-122.
60. Goshima S, Kanematsu M, Watanabe H, et al. Gd-EOB-DTPA enhanced MR imaging: prediction of hepatic fibrosis stages using liver contrast enhancement index and liver-to-spleen volumetric ratio. *J Magn Reson Imaging*. 2012; 36(5): 1148-1153.